JACS
JOURNAL OF THE AMERICAN CHEMICAL SOCIETY

Article

pubs.acs.org/JACS

Four-Coordinate Cobalt Pincer Complexes: Electronic Structure Studies and Ligand Modification by Homolytic and Heterolytic Pathways

Scott P. Semproni,[†] Carsten Milsmann,[†] and Paul J. Chirik*

Department of Chemistry, Princeton University, Princeton, New Jersey 08544, United States

Supporting Information

ABSTRACT: A family of cobalt chloride, methyl, acetylide and hydride complexes bearing both intact and modified *tert*-butyl substituted bis(phosphino)pyridine pincer ligands has been synthesized and structurally characterized and their electronic structures evaluated. Treatment of the unmodified compounds with the stable nitroxyl radical, TEMPO (2,2,6,6-tetramethylpiperidin-1-yloxidanyl) resulted in immediate H-atom abstraction from the benzylic position of the chelate yielding the corresponding modified pincer complexes, (^{tBu}mPNP)CoX (X = H, CH_3, Cl, CCPh). Thermolysis of the methyl and hydride derivatives, (^{tBu}PNP)$CoCH_3$ and (^{tBu}PNP)CoH, at 110 °C also resulted in pincer modification by H atom loss while the chloride and acetylide derivatives proved inert. The relative ordering of benzylic C−H bond strengths was corroborated by H atom exchange experiments between appropriate intact and modified pincer complexes. The electronic structures of the modified compounds, (^{tBu}mPNP)CoX were established by EPR spectroscopy and DFT computations and are best described as low spin Co(II) complexes with no evidence for ligand centered radicals. The electronic structures of the intact complexes, (^{tBu}PNP)CoX were studied computationally and bond dissociation free energies of the benzylic C−H bonds were correlated to the identity of the X-type ligand on cobalt where pure σ donors such as hydride and methyl produce the weakest C−H bonds. Comparison to a rhodium congener highlights the impact of the energetically accessible one-electron redox couple of the first row metal ion in generating weak C−H bonds in remote positions of the supporting pincer ligand.

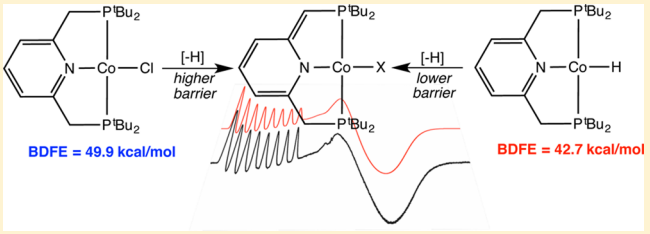

INTRODUCTION

Neutral tridentate, "pincer" type chelates have emerged as a privileged class of ligands due to their widespread use in homogeneous catalysis and small molecule activation processes.[1−8] Base metal catalysis is no exception as pincer ligated iron and cobalt complexes are prevalent motifs with a diverse range of applications from energy science to asymmetric catalysis.[9,10] At the core of many of these applications is metal−ligand cooperativity, whereby redox or chemical events between the transition metal and an ancillary ligand work in concert. This concept is now established as a key mechanistic component of iron-[11−16] and ruthenium-catalyzed hydrogenation of carbonyl compounds,[17,18] iridium-[19] and iron-catalyzed[20] CO_2 hydrogenation to formate, and the ruthenium-catalyzed dehydrogenation of alcohols to esters, amides and imines[21,22] and dehydrogenation of ammonia-borane.[23]

Our laboratory has been interested in the application of iron and cobalt complexes containing redox-active ligands, those that undergo reversible electron transfer events with the transition metal,[24,25] to catalysis. Aryl-substituted bis(imino)-pyridine cobalt methyl complexes,[26] (^{Ar}PDI)$CoCH_3$ are exemplary as well-established redox-active compounds best described as having low-spin Co(II) centers engaged in antiferromagnetic coupling interactions with chelate-centered radical anions (Figure 1).[27,28] Compounds with this electronic

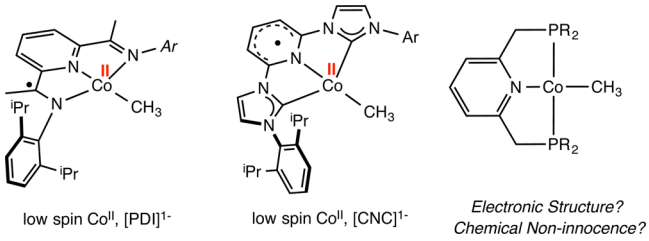

Figure 1. Electronic structures of cobalt methyl complexes bearing tridentate pincer ligands.

structure are active precatalysts for alkene hydrogenation,[29] including asymmetric variants,[10] as well as for alkene hydroboration.[30] With this class of compounds, introduction of electron-donating groups into bis(imino)pyridine iron and cobalt catalysts increased activity in alkene hydrogenation,[31] hydrosilylation,[32] and hydroboration.[30]

Inspired by these observations in iron and cobalt catalysis where more electron-donating ligands improved catalytic performance, aryl-substituted bis(arylimidazol-2-ylidene)-pyridine cobalt alkyl complexes, (^{Ar}CNC)$CoCH_3$, with more

Received: April 30, 2014
Published: June 4, 2014

   dx.doi.org/10.1021/ja504334a | *J. Am. Chem. Soc.* 2014, 136, 9211−9224

electron-donating pyridine dicarbene ligands,[33] were studied. These compounds are highly active precatalysts for the hydrogenation of sterically demanding, unactivated alkenes such as *trans*-methylstilbene, 1-methyl-1-cyclohexene, and 2,3-dimethyl-2-butene, representing one of the most active cobalt hydrogenation catalysts reported to date.[34] A combination of structural, spectroscopic, and computational studies established that the pincer ligands in (^{Ar}CNC)CoCH$_3$ compounds are also redox-active, and the complexes are best described as low-spin cobalt(II) compounds engaged in antiferromagnetic coupling with one electron reduced bis(arylimidazol-2-ylidene)pyridine chelates to account for the observed diamagnetic ground states (Figure 1). Alkyl and hydride migration to the 4-position of the central pyridine provided experimental support for this view of the electronic structure. These results in conjunction with the alkene, ketone, and imine hydrogenation activity reported by Hanson and co-workers with amine-based PNP pincer ligated cobalt complexes,[35−37] suggested that four-coordinate cobalt alkyl complexes supported by pincer ligands offer the opportunity to exploit metal−ligand cooperativity and enable new reactivity and catalytic chemistry.

Neutral, tridentate meridionally coordinating bis(phosphino)pyridine ("PNP") pincer ligands[38] are among the most widely studied and aptly demonstrated examples for metal−ligand cooperativity in homogeneous catalysis. The acidity of the methylene spacers in the benzylic positions of the ligands often results in facile deprotonation and enables the dearomatization−aromatization behavior that is the origin of the chemical noninnocence observed during catalytic turnover.[39−41] One open question surrounding this class of pincers is their redox activity and ability to undergo reversible one electron transfer with a first row transition metal. The presence of a central pyridine ligand, much like in the CNC complexes, may be the origin of such behavior. It is well established that C−H bonds adjacent to organic radicals are significantly weakened as compared to those in the parent closed-shell molecule,[42] suggesting that one electron reduction of PNP-type pincer ligands may lead to *chemical* noninnocence.

In 2006, our laboratory reported the synthesis and spectroscopic investigations of reduced [(^{iPr}PNP)Fe] compounds.[43] Our results, in conjunction with those of Goldman and co-workers, established these complexes as more electron rich as compared to analogous bis(imino)pyridine and bis(arylimidazol-2-ylidene)pyridine iron complexes but obtained no evidence to suggest a redox-active pincer.[43−46] In line with these observations, we recently reported the synthesis of a related cobalt alkyl complex, (^{iPr}PNP)CoCH$_2$SiMe$_3$ and its propensity to undergo two-electron reactivity such as the oxidative addition of H_2 and the C−H bonds of terminal alkynes and arenes to provide rare examples of organometallic Co(III) complexes derived from oxidative addition (Scheme 1).[47,48] Extending this chemistry to boranes, including HBPin and B_2Pin_2 (Pin = pinacolato), resulted in highly active catalysts for the C−H borylation of arenes and various heterocycles,[49] suggesting that changes in preferred electronic structure may enable new catalytic chemistry.

The two-electron chemistry enabled by the [(^{R}PNP)Co] platform contrasts a recent communication by Milstein and co-workers who reported the kinetic instability of (^{R}PNP)CoCH$_3$ toward loss of an H atom from the benzylic position of the pincer ligand (Scheme 2).[50] The resulting cobalt methyl complex with a modified pincer, (^{R}mPNP)CoCH$_3$ has an S = 1/2 ground state and was described as having a ligand based

Scheme 1. Oxidative Addition Reactivity of (^{iPr}PNP)CoCH$_3$ As a Route to Co(III) Complexes

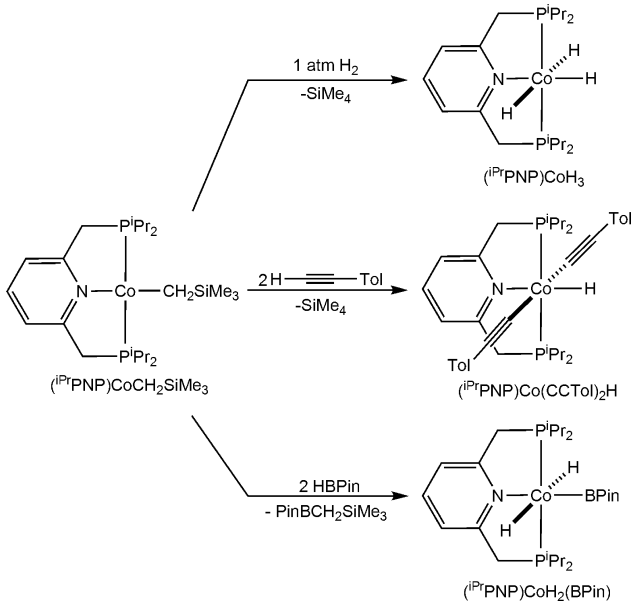

SOMO suggesting that following H atom loss, the pincer supports an organic radical. As an alternative possibility, concomitant intramolecular metal-to-ligand one-electron transfer could lead to a modified pincer that adopts a closed-shell anionic form, resulting in a low spin Co(II) center and, hence, a metal-based SOMO. This view of the electronic structure is frequently encountered with second and third row transition metals.[2,41]

These discrepancies raised several questions for future study such as: (i) What are the electronic structures of cobalt halide complexes with the modified pincer ligands? (ii) Can alkyl complexes with intact PNP pincers be isolated and what effect does the X-type ligand coordinated to cobalt have on the stability of the compounds? (iii) Under what conditions does ligand modification occur and are homolytic versus heterolytic pathways dominant? To answer these questions, a systematic study of the electronic structures of four coordinate cobalt halide, alkyl, and hydride complexes bearing both intact and modified pincer ligands has been carried out. Specifically, the preparation and structural characterization of cobalt halide, alkyl, acetylide, and hydride derivatives is described. Systematic studies into the origin and pathways of H atom loss from the benzylic positions of the pincer were conducted and the bond dissociation free energies as a function of X-type ligand were computed and experimentally evaluated. The electronic structures of the resulting cobalt products with modified pincers have also been studied to distinguish between ligand and metal centered radicals. Comparisons to a rhodium congener are made and highlight the unique role of the base metal and its accessible one electron chemistry in enabling metal−ligand cooperativity.

RESULTS AND DISCUSSION

Synthesis and Characterization of [(^{tBu}PNP)Co] Chloride, Alkyl, and Hydride Compounds. Our studies commenced with the synthesis of chloride, methyl, and hydride complexes of the *tert*-butyl variant of the PNP pincer. This specific substitution was chosen to compare the reaction

dx.doi.org/10.1021/ja504334a | J. Am. Chem. Soc. 2014, 136, 9211−9224

Scheme 2. Ligand Modification via Proposed H-Atom Loss from (^{R}PNP)CoCH$_3$ Compounds As Previously Reported (R = ^{i}Pr, ^{t}Bu).[50]

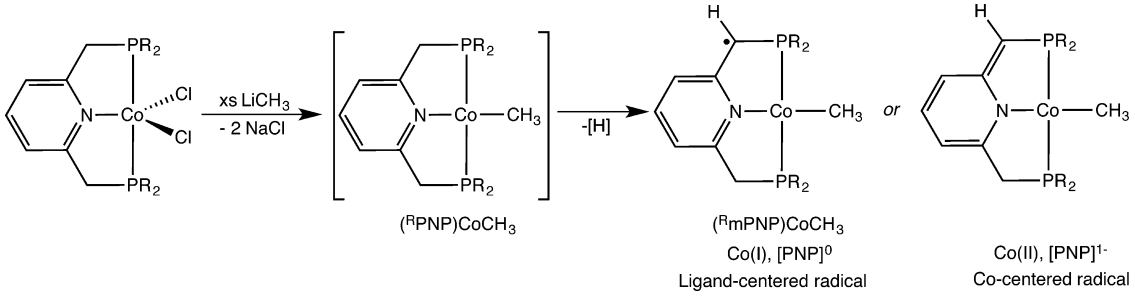

Scheme 3. Synthesis of (^{tBu}PNP)CoCl, (^{tBu}PNP)CoCH$_3$, and (^{tBu}PNP)CoH

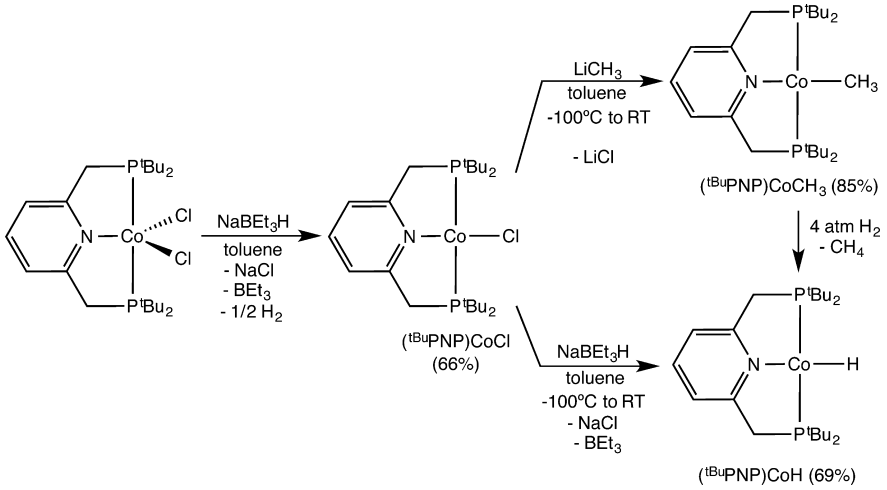

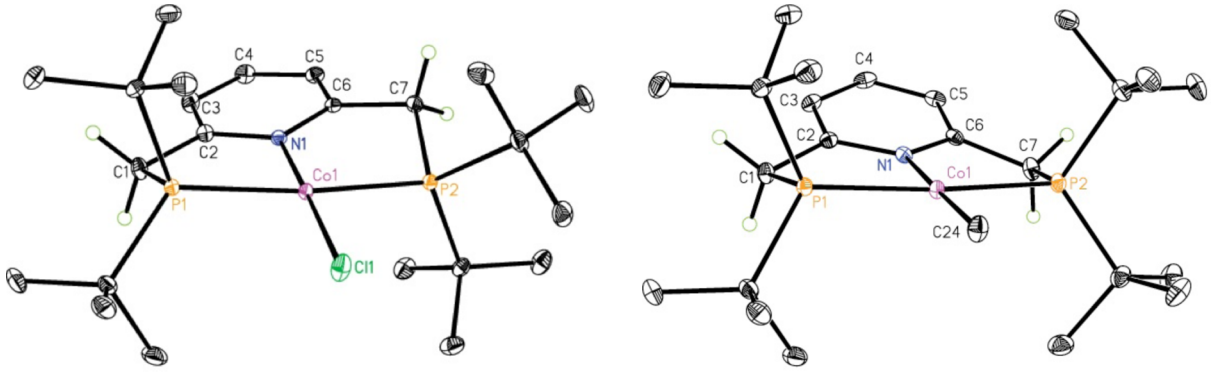

Figure 2. Representation of the molecular structures of (^{tBu}PNP)CoCl (left) and (^{tBu}PNP)CoCH$_3$ (right) with 30% probability ellipsoids. Hydrogens, except those on the benzylic positions, are omitted for clarity.

chemistry with our previous studies with (^{iPr}PNP)CoX compounds and because Milstein and co-workers previously reported improved thermal stability for the methyl derivative, (^{tBu}PNP)CoCH$_3$.[50] The synthetic route used to prepare (^{tBu}PNP)CoCl, (^{tBu}PNP)CoCH$_3$, and (^{tBu}PNP)CoH is detailed in Scheme 3. As reported for the isopropyl variant,[47] treatment of a toluene suspension of (^{tBu}PNP)CoCl$_2$ with one equivalent of NaBEt$_3$H followed by filtration and recrystallization furnished (^{tBu}PNP)CoCl as a red-brown solid in 66% isolated yield. The benzene-d_6 ^{1}H, ^{13}C, and ^{31}P NMR spectra exhibit the number of resonances for a diamagnetic C_{2v} symmetric compound, confirming that the pincer ligand remains intact and has not undergone modification. The observed diamagnetism contrasts the S = 1 magnetic ground state observed for (^{iPr}PNP)CoCl and is likely a result of the enforcement of a planar geometry imparted by the large *tert*-butyl substituents (vide infra).

The solid state structure of (^{tBu}PNP)CoCl was determined by X-ray diffraction and a representation of the molecule is presented in Figure 2. Selected metrical parameters are reported in Table 1. The overall molecular geometry is best described as distorted planar with one of the phosphine ligands lifted slightly above the idealized metal−ligand plane. The N(1)−Co(1)−Cl(1) bond angle of 178.36(3)° is nearly linear while the P(1)−Co(1)−P(2) angle is comparatively large at 172.086(12)°. This contrasts the nearly tetrahedral geometry observed with (^{iPr}PNP)CoCl[47] and suggests that the planarity of (^{tBu}PNP)CoCl is a result of the steric profile of the

dx.doi.org/10.1021/ja504334a | J. Am. Chem. Soc. 2014, 136, 9211−9224

Table 1. Selected Bond Distances (Å) and Angles (Deg) for (^{tBu}PNP)CoCl, (^{tBu}PNP)CoCH$_3$, (^{tBu}PNP)CoH, and (^{tBu}PNP)CoCCPh

	(^{tBu}PNP)CoCl	(^{tBu}PNP)CoCH$_3$	(^{tBu}PNP)CoH	(^{tBu}PNP)CoCCPh
Co(1)−Cl(1)/C(24)	2.2490(6)	1.9994(13)		1.8579(12)
Co(1)−N(1)	1.8972(10)	1.9033(10)	1.889(5)	1.9103(10)
Co(1)−P(1)	2.1912(9)	2.1834(4)	2.127(2)	2.1574(3)
Co(1)−P(2)	2.1868(9)	2.1816(4)	2.127(2)	2.1599(3)
C(2)−C(3)	1.3896(18)	1.3793(17)	1.377(11)	1.3862(16)
C(3)−C(4)	1.3817(19)	1.3945(19)	1.405(11)	1.3856(18)
C(4)−C(5)	1.3819(19)	1.392(2)	1.385(11)	1.3875(18)
C(5)−C(6)	1.3816(17)	1.3796(18)	1.391(10)	1.3861(16)
N(1)−C(2)	1.3740(16)	1.3892(16)	1.387(9)	1.3785(14)
N(1)−C(6)	1.3863(16)	1.3909(15)	1.383(9)	1.3807(14)
C(1)−C(2)	1.4983(18)	1.4974(17)	1.502(10)	1.5013(16)
C(6)−C(7)	1.5007(17)	1.4977(18)	1.505(10)	1.4996(16)
N(1)−Co(1)−Cl(1)/C(24)	178.36(3)	178.76(5)		178.25(4)
P(1)−Co(1)−P(2)	172.086(12)	172.942(14)	173.20(8)	174.557(13)

Figure 3. Representation of the molecular structures of (^{tBu}PNP)CoH (left) and (^{tBu}PNP)CoCCPh (right) at 30% probability ellipsoids. Hydrogens, except those on the benzylic postions and the cobalt-hydride, are omitted for clarity.

phosphine substituents where the larger *tert*-butyl groups inhibit the chloride ligand from distorting from the idealized metal−ligand plane.

Methylation of (^{tBu}PNP)CoCl was accomplished by treatment with one equivalent of a 1.6 M diethyl ether solution of LiCH$_3$ at −100 °C and warming to ambient temperature followed by recrystallization (Scheme 3). This procedure furnished (^{tBu}PNP)CoCH$_3$ as dark brown crystals in 85% yield and the NMR spectroscopic features are identical to those previously reported by Milstein.[50] To our knowledge, the solid-state structure of (^{tBu}PNP)CoCH$_3$ has not been reported. X-ray quality crystals of the compound were obtained from a diethyl ether solution stored at −35 °C. A representation of the molecular structure is reported in Figure 2 and established an overall idealized planar geometry about the cobalt. Selected bond distances are reported in Table 1.

The preparation of (^{tBu}PNP)CoH was also explored (Scheme 3). Addition of NaBEt$_3$H to a toluene solution of (^{tBu}PNP)-CoCl followed by filtration and recrystallization yielded red-brown crystals identified as (^{tBu}PNP)CoH in 69% yield. This compound was also prepared by addition of 4 atm of H$_2$ to (^{tBu}PNP)CoCH$_3$. With the isopropyl variant, addition of 4 atm of H$_2$ to (^{iPr}PNP)CoCH$_3$ resulted in loss of methane and isolation and crystallographic characterization of a rare example of a Co(III) trihydride, (^{iPr}PNP)CoH$_3$.[47] The benzene-d_6 ^{1}H NMR spectrum of (^{tBu}PNP)CoH exhibited a triplet ($^2J_{PH}$ = 65.3 Hz) at −29.0 ppm assigned as the cobalt-hydride resonance. A single ^{31}P NMR signal was observed at 85.2 ppm, corroborating formation of a diamagnetic C_{2v} symmetric product. A medium intensity band was also identified at 1746 cm^{-1} in the solid-state (KBr) infrared spectrum, consistent with a terminal cobalt-hydride.[51]

The solid state structure of (^{tBu}PNP)CoH was determined by X-ray diffraction. A representation of the molecule is presented in Figure 3 and selected bond distances and angles are reported in Table 1. The hydride ligand was located in the difference map. As with the chloride and methyl derivatives, (^{tBu}PNP)-CoH is planar. The metrical parameters of the cobalt-pincer linkages are similar to those observed for (^{tBu}PNP)CoCl. Notably, introduction of larger *tert*-butyl substituents on the phosphines of the pincer stabilize the cobalt(I) hydride; the corresponding isopropyl-substituted compound, (^{iPr}PNP)CoH, has thus far eluded observation due to rapid decomposition by P−C bond cleavage of the pincer. Placing a benzene-d_6 solution of (^{tBu}PNP)CoH under four atmospheres of H$_2$ resulted in broadening of the hydride signal into the baseline and no observation of free dihydrogen in solution. The methylene hydrogens shift downfield to 2.46 ppm and the *para*-pyridine upfield to 7.79 ppm. Both values approach those observed for (^{iPr}PNP)CoH$_3$,[47] suggesting (^{tBu}PNP)CoH$_3$ is formed and exchanges with (^{tBu}PNP)CoH. Even higher pressures of H$_2$ may allow observation of (^{tBu}PNP)CoH$_3$, conditions not conveniently or safely accessed in standard NMR tubes.

dx.doi.org/10.1021/ja504334a | J. Am. Chem. Soc. 2014, 136, 9211−9224

The cobalt acetylide, (^{tBu}PNP)CoCCPh was prepared by addition of the terminal alkyne to a benzene-d_6 solution of (^{tBu}PNP)CoH. The desired product was isolated as diamagnetic, red-brown crystals in 94% yield and characterized by multinuclear NMR spectroscopy and X-ray diffraction (eq 1). No evidence was obtained for alkyne insertion products.

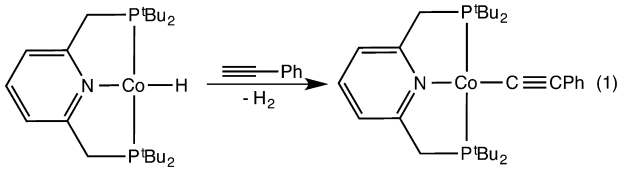

(^{tBu}PNP)CoH (^{tBu}PNP)CoCCPh (94%)

The electronic properties of the series of (^{tBu}PNP)CoX compounds were investigated by cyclic voltammetry (CV). In a standard experiment, a 1 mM solution of the cobalt compound was prepared in tetrahydrofuran with 0.1 M of [NBu_4][PF_6] as electrolyte. The obtained CVs are presented in Figure 4. At 100

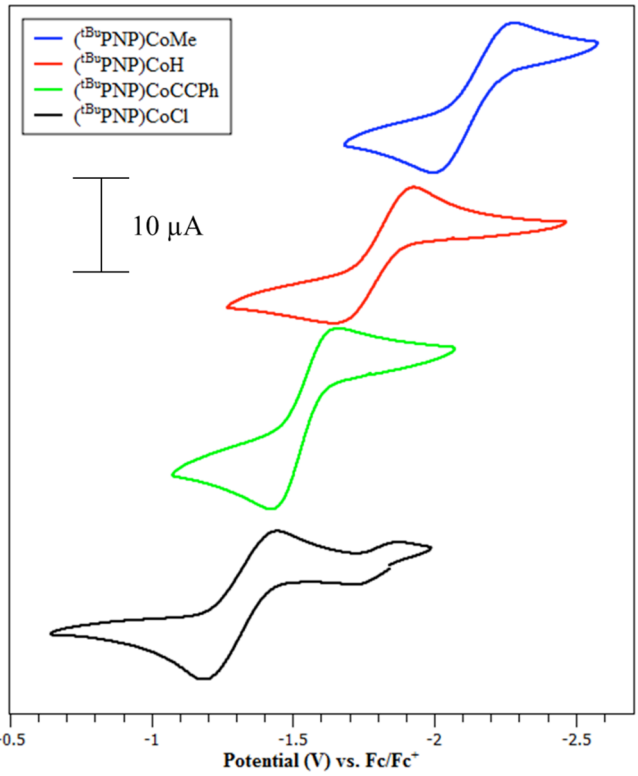

Figure 4. Cyclic voltammagrams of (^{tBu}PNP)CoX complexes in tetrahydrofuran with 0.1 M [NBu_4][PF_6] as electrolyte and 100 mV/s scan rate.

mV/s scan rate, all complexes display a single reversible wave assigned as the Co(I)/Co(II) redox couple. The measured redox potentials for the four compounds are presented in Table 2. Consistent with the relative electron density at the Co(I) center in each complex, the compounds become progressively easier to oxidize as we move from (^{tBu}PNP)CoCl to (^{tBu}PNP)$CoCH_3$. Milstein and co-workers have reported the electrochemistry of (^{tBu}PNP)RhCl in acetone and located the Rh(I)/Rh(II) redox couple at 0.37 V vs Fc/Fc^+, shifted by over 1.6 V from the analogous cobalt complex.[52]

Exploration of Ligand Modification: Heterolytic and Homolytic C−H Bond Cleavage. The isolation of (^{tBu}PNP)-

Table 2. Measured Redox Potentials for (^{tBu}PNP)CoX Compounds

compound	$E°$ (V vs Fc/Fc^+)
(^{tBu}PNP)CoCl	−1.32
(^{tBu}PNP)CoCCPh	−1.54
(^{tBu}PNP)CoH	−1.79
(^{tBu}PNP)$CoCH_3$	−2.14

$CoCH_3$ in this study and thermal stability of (^{iPr}PNP)$CoCH_3$ reported in our prior work[47] contrasts Milstein's claim that complexes of this type are kinetically unstable toward spontaneous H atom loss.[50] Because it is well established that PNP-based pincer ligands often have acidic methylene spacers,[39] heterolytic C−H bond cleavage by deprotonation of the benzylic positions of (^{tBu}PNP)CoCl was explored. Addition of one equivalent of NaO^{t}Bu to a THF solution of (^{tBu}PNP)CoCl at −35 °C followed by removal of the volatiles and extraction of the product into pentane yielded red crystals identified as the cobalt dinitrogen complex, (^{tBu}mPNP)CoN_2, with a modified pincer ligand (eq 2). Similar chemistry has previously been reported for the analogous bis(imino)pyridine cobalt chloride compound where treatment with KO^{t}Bu resulted in deprotonation of an imine methyl group with concomitant salt elimination and yielded the modified cobalt dinitrogen complex.[28,53] The rhodium congener of (^{tBu}mPNP)-CoN_2 has also been isolated by Goldberg and co-workers from treatment of [(^{tBu}PNP)RhN_2][OTf] with strong bases such as $LiCH_3$ or KO^{t}Bu in THF.[41] Proton transfer from the benzylic positions was also used to account for isotopic exchange with D_2 gas in related PNP-pincer iridium phenyl complexes.[54]

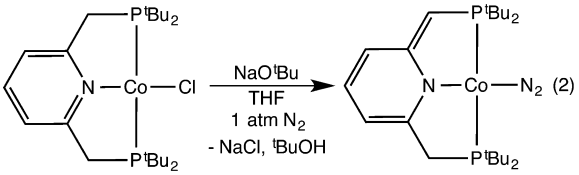

(^{tBu}mPNP)CoN_2

The diamagnetic cobalt dinitrogen complex was characterized by a combination of multinuclear NMR and IR spectroscopies as well as X-ray diffraction. A strong N−N stretch was observed at 2021 cm^{-1} for the coordinated dinitrogen ligand. The solid-state structure, presented in Figure 5, confirms the identity of the molecule as an essentially planar,

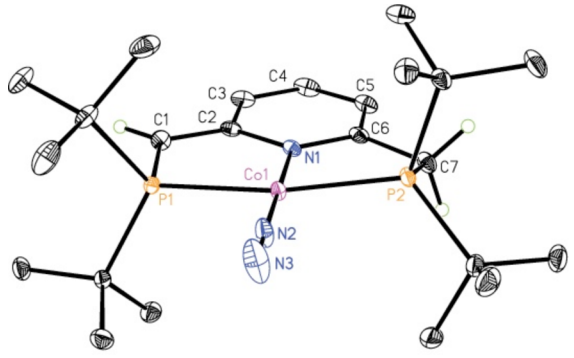

Figure 5. Representation of the molecular structure of (^{tBu}mPNP)-CoN_2 at 30% probability ellipsoids. Hydrogen atoms, except on benzylic positions, are omitted for clarity. Only one crystallographically independent molecule is shown.

dx.doi.org/10.1021/ja504334a | J. Am. Chem. Soc. 2014, 136, 9211−9224

cobalt(I) dinitrogen compound. This electronic structure is confirmed by DFT calculations. A qualitative MO diagram is shown in Supporting Information Figure S3. Selected bond distances and angles are reported in Table 3. The metrical parameters of the solid state structure clearly demonstrate the dearomatization of the pyridine ring, with alternating bond lengths of C(2)−C(3) (1.437(2) Å), C(3)−C(4) (1.360(2) Å), C(4)−C(5) (1.406(2) Å), and C(5)−C(6) (1.374(2) Å). The difference between the benzylic C−C bond lengths of C(1)−C(2) (1.378(2) Å) and C(6)−C(7) (1.499(2) Å) indicate the presence of a monoanionic chelate. The facile deprotonation associated with (^{tBu}PNP)CoCl established the acidity of the methylene positions of the PNP positions when coordinated to a reduced cobalt center, suggesting heterolytic C−H bond cleavage pathways are possible in the formation of modified chelates similar to known rhodium complexes.

Table 3. Selected Bond Distances (Å) and Angles (Deg) for (^{tBu}mPNP)CoN$_2$, (^{tBu}mPNP)CoCl, and (^{tBu}mPNP)CoH

	(^{tBu}mPNP)CoN$_2$	(^{tBu}mPNP)CoCl	(^{tBu}mPNP)CoH
Co(1A)-N(1)	1.9439(12)	1.962(5)	1.953(6)
Co(1A)-P(1)	2.2240(4)	2.248(6)	2.1999(16)
Co(1A)-P(2A)	2.1975(4)	2.264(13)	2.1999(16)
Co(1A)-Cl(1A)		2.197(7)	
C(2)−C(3)	1.437(2)	1.420(3)	1.411(7)
C(3)−C(4)	1.360(2)	1.362(3)	1.385(7)
C(4)−C(5)	1.406(2)	1.395(3)	1.385(7)
C(5)−C(6)	1.374(2)	1.382(3)	1.411(7)
N(1)−C(2)	1.4049(18)	1.390(2)	1.388(7)
N(1)−C(6)	1.3714(17)	1.380(3)	1.388(7)
C(1)−C(2)	1.378(2)	1.399(3)	1.41(2)
C(6)-C(7A)	1.499(2)	1.459(13)	1.52(3)
P(1)-Co(1A)-P(2A)	169.688(16)	167.9(3)	174.36(9)

Because of the reported H atom loss chemistry from (^{R}PNP)CoCH$_3$ complexes,[50] homolytic pathways for modification of the PNP ligand were also explored. The isolation of a family of alkyl, chloride, acetylide, and hydride complexes allows for the systematic study of homolytic C−H bond scission as a function of the X-type ligand in the cobalt coordination sphere. Milstein has previously reported that addition of TEMPO to (^{iPr}PNP)CoCH$_3$ resulted in H atom abstraction and formed (^{iPr}mPNP)CoCH$_3$ and TEMPO-H, establishing a homolytic bond dissociation energy of less than 67 kcal/mol for the methylene positions of the PNP pincer.[55] Similar experiments were conducted with (^{tBu}PNP)CoCl, (^{tBu}PNP)CoH, and (^{tBu}PNP)CoCCPh and cleanly yielded the corresponding (^{tBu}mPNP)CoX derivatives in good to high yield in each case (eq 3).

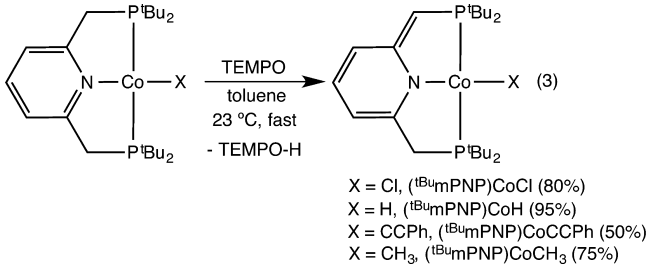

All three modified pincer cobalt complexes are paramagnetic with effective magnetic moments consistent with $S = 1/2$ ground states. Each compound exhibits relatively sharp ^{1}H NMR spectra in benzene-d_6 solution at 23 °C with the number of paramagnetically shifted resonances consistent with C_s symmetric compounds with a mirror plane of symmetry that contains the idealized metal-chelate plane. Two examples, (^{tBu}mPNP)CoCl and (^{tBu}mPNP)CoH were characterized by X-ray diffraction and representations of the molecular structures are presented in Figure 6. Although the hydrogens on the pincer ligand were located in both cases and confirmed ligand modification, the Co−H of (^{tBu}mPNP)CoH was not. A medium intensity band was located at 1819 cm^{-1} in the solid-state infrared spectrum of the compound, establishing the presence of the Co−H. In both structures, the C(1)−C(2) distances of 1.399(3) (Cl) and 1.41(2) (H) Å are significantly shorter than the values of 1.459(13) and 1.52(3) Å for the corresponding $C_{ipso}-C_{methylene}$ positions, signaling ligand modification. Alternating bond lengths are also observed in the pyridine rings, indicating dearomatization (Table 3).

Each of the (^{tBu}mPNP)CoX compounds was additionally characterized by X-band EPR spectroscopy. The electronic structure of (^{iPr}mPNP)CoCH$_3$ was previously described as a low spin Co(I) compound with a ligand-centered radical arising from a redox-active modified pincer.[50] Throughout the manuscript, we have represented the modified pincer as an anionic ligand thereby rendering the metal as low-spin Co(II) to accommodate the measured magnetic data. For all complexes, the obtained magnetic moments are significantly

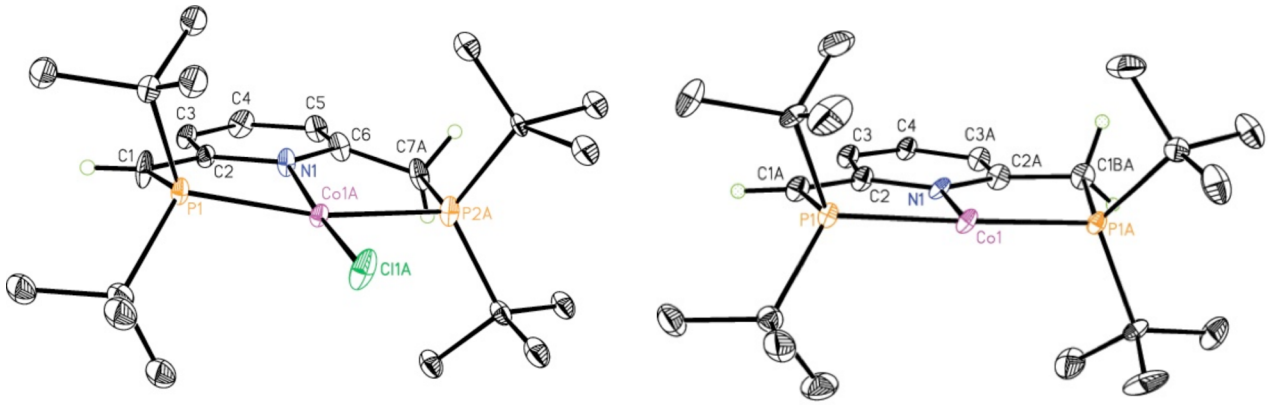

Figure 6. Representation of the molecular structure of (^{tBu}mPNP)CoCl (left) and (^{tBu}mPNP)CoH (right) at 30% probability ellipsoids. Hydrogen atoms, except on benzylic positions, are omitted for clarity. Only one of two disordered orientations of each molecule is shown.

dx.doi.org/10.1021/ja504334a | J. Am. Chem. Soc. 2014, 136, 9211−9224

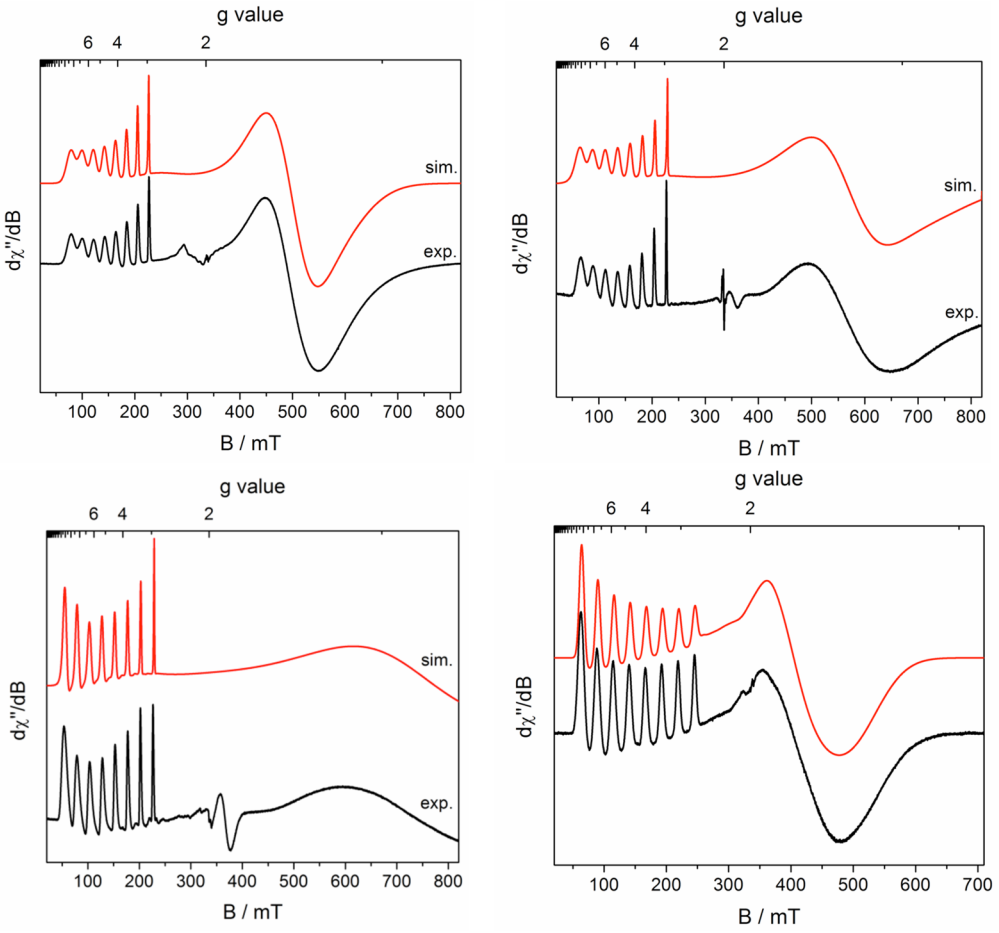

Figure 7. EPR spectra of (^{iPr}mPNP)CoCH$_3$ (upper left), (^{tBu}mPNP)CoCl (upper right), (^{tBu}mPNP)CoCH$_3$ (lower left), and (^{tBu}mPNP)CoH (lower right). Each spectrum was recorded in toluene/diethyl ether glass at 10 K. Conditions for (^{iPr}mPNP)CoCH$_3$, microwave frequency = 9.384 GHz, power = 0.63 mW, modulation amplitude = 1 mT/100 kHz. Conditions for (^{tBu}mPNP)CoCl, microwave frequency = 9.384 GHz, power = 0.63 mW, modulation amplitude = 1 mT/100 kHz. Conditions for (^{tBu}mPNP)CoH, microwave frequency = 9.375 GHz, power = 2.00 mW, modulation amplitude = 1 mT/100 kHz. Conditions for (^{tBu}mPNP)CoCH$_3$, microwave frequency = 9.379 GHz, power = 0.63 mW, modulation amplitude = 1 mT/100 kHz.

higher than the spin-only value expected for S = 1/2 compounds, indicating significant contributions from spin−orbit coupling. The two descriptions differ by the parentage of the SOMO (Scheme 2); in the published case, the unpaired spin is pincer-based, which should result in small orbital contributions to the magnetic moment, whereas in the latter, the electron is metal-centered opening a pathway for strong spin−orbit coupling.

Measurements were initially conducted in toluene solution at ambient temperature as organic radicals are typically observed under these conditions. No signal was observed for any (^{R}mPNP)CoX compound at this temperature. However, preparing samples of each compound in toluene−diethyl ether glasses and subsequent cooling to 10 K produced the spectra presented in Figure 7. In each case, an axial signal was observed with one large g value at approximately g = 4.3−4.5, which is split into eight lines due to hyperfine coupling to the ^{59}Co nucleus (I = 7/2, 100% natural abundance), and two smaller g values below 2. These signals do not exhibit any resolved hyperfine coupling.

The observation of highly anisotropic signals and very large cobalt hyperfine coupling clearly supports a cobalt rather than [PNP]-based radical and definitively establishes that the modified pincer is a closed-shell, monoanionic ligand. Low-spin cobalt(II) complexes are well known to exhibit highly anisotropic EPR spectra.[56] Tonzetich and co-workers have recently reported similar EPR spectral properties for planar Co(II) complexes bearing *N*-heterocyclic carbenes.[57] The origin of the large g anisotropy is a result of strong spin−orbit coupling arising from a nearly degenerate set of d orbitals in a planar ligand field, which results in large orbital contributions to the electronic g values. A theoretical analysis by Nishida and co-workers demonstrated that both g and A values are highly sensitive to small changes in energy differences between the four low-lying d orbitals in the planar ligand field.[56c] On the basis of these findings, the spectra presented in Figure 7 were readily simulated using the parameters reported in Table 4. Accurate reproduction of the line shapes was accomplished using a combination of g-strain and A-strain parameters to model a distribution of slightly different molecular geometries frozen out upon formation of the solvent glass resulting in highly anisotropic line broadening.

The possibility of thermally induced C−H bond scission was investigated for all four (^{tBu}PNP)CoX compounds (Table 5). Each thermolysis reaction was conducted in benzene-d_6 and monitored by ^{1}H NMR spectroscopy. Both the diamagnetic starting compounds and the paramagnetic products exhibit sharp, readily assigned NMR spectra facilitating determination

dx.doi.org/10.1021/ja504334a | J. Am. Chem. Soc. 2014, 136, 9211−9224

Table 4. Summary of EPR Spectroscopic Parameters for (^{R}mPNP)CoX Compounds[a]

	(^{tBu}mPNP) CoCl	(^{tBu}mPNP) CoMe	(^{iPr}mPNP) CoMe	(^{tBu}mPNP) CoH
g_x	4.50	4.66	4.35	4.30
g_y	1.15	0.75	1.32	1.68
g_z	1.06	0.65	1.15	1.34
A_{xx} (MHz)	1450	1600	1270	1560
A_{strain}	150, 0, 0	70, 0, 0	160, 0, 0	40, 0, 0
g_{strain}	0.26, 0.26, 0.30	0.14, 0.14, 0.14	0.25,0.22,0.31	0.20, 0.30, 0.30

[a] A values reported in MHz.

Table 5. Evaluation of the Thermal Stability of (^{R}PNP)CoX Compounds

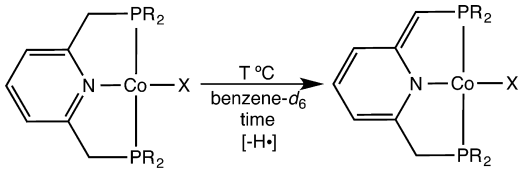

(^{tBu}PNP)CoX (^{tBu}mPNP)CoX

compound	T (°C)	time (hrs)	outcome
(^{tBu}PNP)CoCl	120	24	no reaction
(^{tBu}PNP)CoCCPh	120	24	no reaction
(^{tBu}PNP)CoH	110	16	(^{tBu}mPNP)CoH
(^{tBu}PNP)CoCH$_3$	120	18	(^{tBu}mPNP)CoCH$_3$

of the progress of each reaction. Heating a solution of either (^{tBu}PNP)CoCl or(^{tBu}PNP)CoCCPh to 120 °C for 24 h produced no change. By contrast, heating (^{tBu}PNP)CoCH$_3$ or (^{tBu}PNP)CoH to 110 °C for 18 h resulted in conversion to the corresponding modified compounds. Analysis of the volatile products following (^{tBu}PNP)CoH thermolysis by Toepler pump established formation of H_2 gas as a product of the reaction. Approximately 30% of the expected combustible gas was collected. The fate of the balance of the H atoms is unknown, but a significant quantity of free ligand and metallic cobalt was also observed. Performing the thermolysis of (^{tBu}PNP)CoH on a preparative scale allowed for the isolation of (^{tBu}mPNP)CoH in 46% yield, suggesting decomposition of (^{tBu}PNP)CoX complexes is competitive with H atom loss. It is possible the observed H_2 is a result of an unidentified decomposition process.

Equilibration studies were also conducted to gain additional experimental insight into the relative C−H bond strengths of the benzylic positions of the pincer ligand as a function of the X-type ligand. In each experiment, equimolar mixtures of (^{tBu}mPNP)CoX and (^{tBu}PNP)CoY derivatives were mixed and the propensity to undergo H atom transfer assessed by NMR spectroscopy as both the diamagnetic and paramagnetic compounds are readily observable. A summary of the results of these experiments is reported in Table 6.

Mixing cobalt compounds with two X-type ligands that both undergo thermal H atom loss, (^{tBu}PNP)CoCH$_3$ and (^{tBu}mPNP)CoH, yielded (^{tBu}mPNP)CoCH$_3$ and (^{tBu}PNP)CoH as products. At 23 °C, all four compounds were present in near equal amounts immediately after mixing (Table 6). The same equilibrium mixture was attained from mixing (^{tBu}mPNP)-CoCH$_3$ with (^{tBu}PNP)CoH (Entry 1). Preparation of a combination of compounds where one member undergoes thermal H atom loss, (^{tBu}PNP)CoCH$_3$, with a modified compound that does not, (^{tBu}mPNP)CoCl, resulted in immediate formation of (^{tBu}mPNP)CoCH$_3$ and (^{tBu}PNP)CoCl (Entry 4). Allowing the resulting solution to stand at 23 °C or mixing fresh solutions of the products produced no change, demonstrating the irreversibility of the process. Performing similar experiments with other combinations support the observations from the thermolysis experiments—those compounds that undergo thermal ligand modification undergo H atom transfer to modified complexes that do not (Table 6). These results establish that the compounds with strong field, pure σ-donating X-type ligands such as hydride and methyl have weaker benzylic C−H bonds than analogues with weaker field ligands, such as chloride and acetylide.[58]

To gain additional insight into ligand modification by C−H bond homolysis, attempts were made to measure the kinetic isotope effect for conversion of the pincer complexes into their modified counterparts. These experiments required the deuterated isotopologue, (^{tBu}PNP-d_5)CoD, a compound conveniently prepared by exposure of a benzene-d_6 solution of (^{tBu}PNP)CoH to 4 atm of D_2 for 48 h. The deuteria are located in the four benzylic positions and in the *para* pyridine. Performing a control experiment whereby a benzene-d_6 solution of (^{tBu}PNP)CoH was treated with an equimolar amount of (^{tBu}mPNP-d_4)CoD at 23 °C resulted in immediate (<5 min) exchange of the deuterium and hydrogen between the methylene positions of the two compounds. The converse experiment whereby (^{tBu}PNP-d_5)CoD and (^{tBu}mPNP)CoH were mixed produced an identical result, demonstrating that

Table 6. Ladder Experiments to Establish Experimental Estimates of Pincer C−H Bond Dissociation Free Energies (BDFEs)

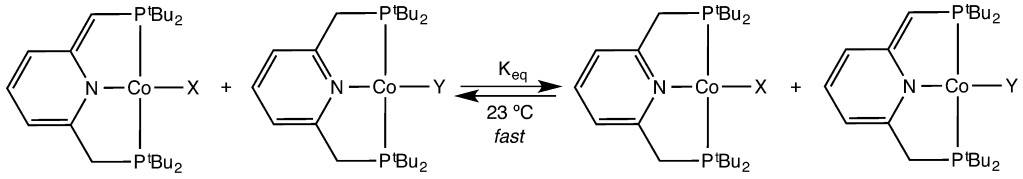

entry	Y	X	K_{eq} (23 °C)
1	H	CH$_3$	~1
2	H	Cl	>100
3	H	CCPh	>100
4	CH$_3$	Cl	>100
5	CH$_3$	CCPh	>100
6	Cl	CCPh	~1

dx.doi.org/10.1021/ja504334a | J. Am. Chem. Soc. 2014, 136, 9211−9224

interpretation of kinetic isotope effect by this method is compromised by "self exchange" between like isotopologues. Notably, the ^{1}H NMR spectra of mixtures of (^{tBu}PNP)CoX and (^{tBu}mPNP)CoX are unperturbed from their consistuent single component spectra, indicating that the H atom self-exchange process, although rapid synthetically, is not observable on the NMR time scale. Attempts to obtain reliable KIE data on the thermolysis of (^{tBu}PNP)CoH to (^{tBu}mPNP)CoH were also frustrated by the rapid self-exchange process as well as from complications from the formation of metallic cobalt and free ligand that accompanied the H atom loss event.

Reaction Chemistry with Alkynes. In Milstein's communication describing spontaneous ligand modification of (^{R}PNP)CoCH$_3$ compounds at ambient temperature,[50] diphenylacetylene was used as a trap of H atoms ejected from the benzylic positions of the pincer and isomers of stilbene were detected. Because our observations demonstrate that C−H bond homolysis does not occur at room temperature and has a much higher barrier, we sought to reconcile this discrepancy. Addition of PhCCPh to a benzene-d_6 solution of either (^{tBu}PNP)CoH or (^{tBu}PNP)CoCH$_3$, resulted in insertion of the alkyne into the cobalt-hydride or alkyl followed by orthometalation of one of the phenyl substituents (eq 4). For the cobalt hydride, the reaction was complete after 18 h at 23 °C, whereas for the cobalt methyl, heating to 60 °C was required and produced significant quantities of free pincer ligand and metallic cobalt as side products. Both products were characterized by multinuclear NMR spectroscopy and the molecular structures were also confirmed by X-ray diffraction. One example, (^{tBu}PNP)Co(C_6H_4−CH═CHPh) is presented in Figure 8. All of the data suggests that one electron, H atom loss chemistry is not operative at ambient temperature and more traditional hydride insertion and two-electron oxidative addition type reactivity is preferred.

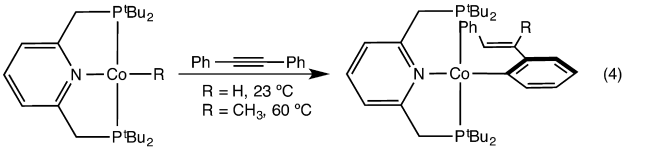

R = H, (^{tBu}PNP)Co(C_6H_4CH=CHPh) (72%)
R = CH$_3$, (^{tBu}PNP)Co(C_6H_4CH=CMePh) (25%)

How then is Milstein's isolation of (^{R}mPNP)CoCH$_3$ compounds explained? Recall that the synthesis of these molecules relied on treatment of (^{R}PNP)CoCl$_2$ with a large (~10 equiv) excess of MeLi.[50] A proposed sequence to account for the observed products is presented in Scheme 4. The sequence begins with *deprotonation* of a C−H bond of the methylene position with LiCH$_3$ to liberate methane and precipitate lithium chloride. Similar reactivity has been observed upon addition of KO^{t}Bu to a related PNN-pincer complex of platinum,[59] PNP derivatives of rhodium,[52] palladium,[60] nickel,[61] copper,[62] and in this work in the synthesis of (^{tBu}mPNP)CoN$_2$ by deprotonation and salt elimination from (^{tBu}PNP)CoCl. Once (^{R}mPNP)CoCl compounds are present, straightforward salt metathesis with LiCH$_3$ yields (^{R}mPNP)CoCH$_3$ (Scheme 4). It is likely that the excess alkylating agents used in the Milstein synthesis accounts for the observation of the modified methyl complexes as heterolytic, deprotonation pathways are preferred and that C−H homolysis reactions are not operative at ambient temperature.

Support for this hypothesis derives from the observation that treatment of (^{tBu}PNP)CoCl$_2$ with 1.5 equiv of NaO^{t}Bu exclusively yielded (^{tBu}mPNP)CoCl, demonstrating the acidity of the benzylic position. Addition of 1 equiv of MeLi to a diethyl ether or benzene slurry of (^{tBu}PNP)CoCl$_2$ also yielded (^{tBu}mPNP)CoCl along with (^{tBu}PNP)CoCl and (^{tBu}mPNP)-CoCH$_3$ as judged by NMR spectroscopy. This experiment demonstrates that MeLi acts as a base for benzylic deprotonation. The observed side products are likely due to the poor solubility of (^{tBu}PNP)CoCl$_2$. Also consistent with the proposal in Scheme 4 is the clean alkylation of isolated (^{tBu}mPNP)CoCl with MeLi to yield (^{tBu}mPNP)CoCH$_3$.

Computational Studies: Electronic Structure of (^{R}mPNP)CoX Compounds. In the original report of the (^{R}mPNP)CoCH$_3$ derivatives, the electronic structure of the S = 1/2 modified complex was described as low spin cobalt(I) with a ligand-centered radical as the SOMO.[50] If such a description is correct, then modified PNP ligands are redox active and potentially offer unique reactivity pathways. The EPR spectra reported in Figure 7 suggest otherwise as signals with large g anisotropy and cobalt hyperfine coupling were observed, consistent with metal-based rather than ligand-based spin. Unrestricted, full molecule DFT calculations were also

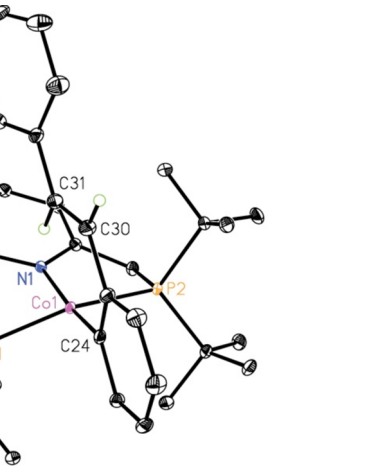

Figure 8. Molecular structure of (^{tBu}PNP)Co(C_6H_4−CH═CHPh) at 30% probability ellipsoids. Hydrogen atoms, except those attached to C30 and C31, are omitted for clarity.

Scheme 4. Proposed Pathway for the Generation of Modified Pincer Complexes from (^{R}PNP)CoCl$_2$ with Excess Methyl Lithium

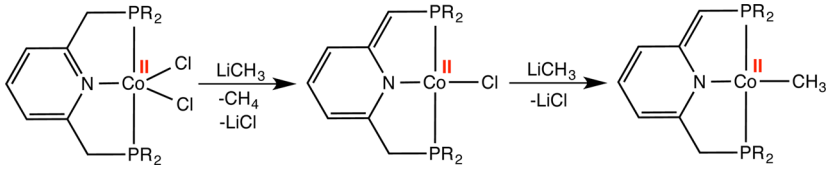

dx.doi.org/10.1021/ja504334a | J. Am. Chem. Soc. 2014, 136, 9211−9224

performed on (^{tBu}mPNP)CoCH$_3$ at the B3LYP level of theory to corroborate the electronic structure proposed based on the EPR data.[63] A qualitative molecular orbital diagram and associated spin density plot corresponding to the optimized structure are presented in Figure 9. The electronic structure

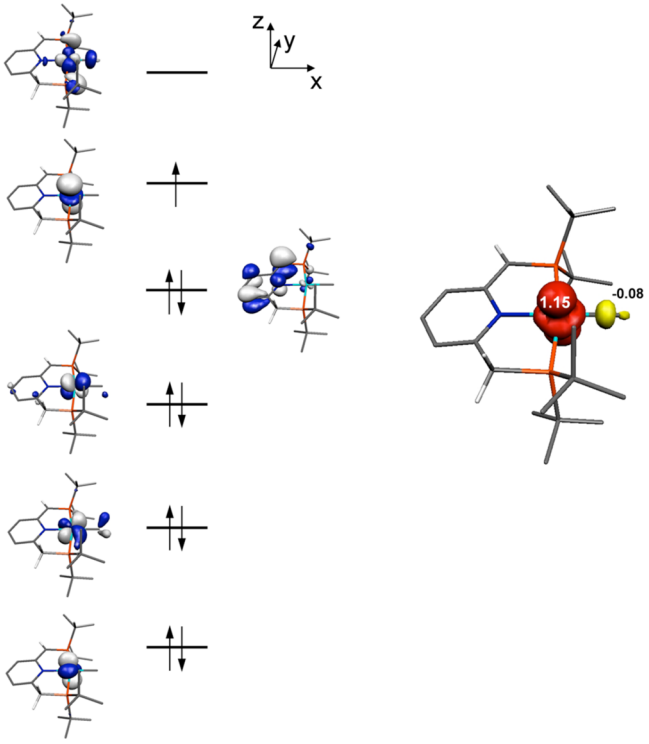

Figure 9. Qualitative molecular orbital diagram (left) and computed spin density plot (right) for (^{tBu}mPNP)CoCH$_3$ at the B3LYP level of DFT.

corresponds to a low spin Co(II) complex with the SOMO of the molecule principally a d_{z^2} molecular orbital on the metal. The Mulliken spin density plot confirms this view of the electronic structure with almost all of the unpaired spin in the molecule located on the cobalt center. The highest doubly occupied orbital is principally ligand-based, further supporting a closed-shell form of the modified pincer. Importantly, there is no unpaired spin density on the pincer ligand. Analogous calculations for the remaining complexes (^{tBu}mPNP)CoX (X = H, Cl, CCPh) produced the same electronic structure.

Electronic Structure of (^{R}PNP)CoX Compounds and Computation of Benzylic C–H Bond Dissociation Free Energies (BDFEs) as a Function of the X-Type Ligand. The electronic structure of the family of (^{tBu}PNP)CoX (X = Cl, C≡CPh, Me, H) compounds was also explored to determine (i) if the PNP in its unmodified form can support ligand centered radicals and (ii) if there is a correlation between preferred electronic ground state and propensity to undergo H atom loss. Generation of a PNP radical anion was initially targeted to determine under what, if any, conditions the chelate could be reduced. Cyclic voltammetry of the free ligand, ^{tBu}PNP showed no oxidation or reduction waves in the THF solvent window. Chemical reduction of the free pincer was accomplished by stirring a THF solution of ^{tBu}PNP with excess sodium metal and the resulting radical anion was characterized by EPR spectroscopy at ambient temperature (Supporting Information Figure S4), demonstrating that such species are chemically accessible with sufficiently potent reductants.

The S = 0 ground states for the (^{tBu}PNP)CoX compounds present an experimental challenge for establishing the redox activity of the pincer. Comparison of the metrical parameters of the crystallographically characterized cobalt compounds to those with pincers undoubtedly in their neutral form, (e.g., (^{iPr}PNP)FeBr$_2$) revealed no statistically significant differences in the bond lengths in the central pyridine ring. No anomalous ^{1}H NMR shifts were observed.[34] Because of these experimental challenges, we relied on the output of DFT calculations for electronic structure determination. Full molecule geometry optimization computations on (^{tBu}PNP)CoCl and (^{tBu}PNP)-CoCCPh established preferred closed-shell singlet ground states corresponding to traditional low-spin Co(I), d^8 complexes with redox innocent pincers. A representative qualitative molecular orbital diagram for (^{tBu}PNP)CoCl is presented in the left portion of Figure 10, and that for (^{tBu}PNP)CoCCPh is reported in Supporting Information Figure S1.

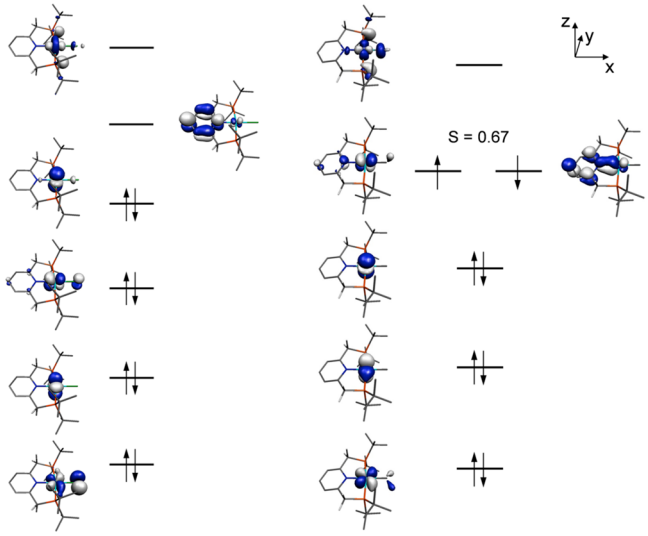

Figure 10. DFT-computed qualitative molecular orbital diagrams for (^{tBu}PNP)CoCl (left) and (^{tBu}PNP)CoCH$_3$ (right).

Analogous computations on both (^{tBu}PNP)CoCH$_3$ and (^{tBu}PNP)CoH produced broken symmetry solutions that are best described as low-spin Co(II), d^7 complexes engaged in antiferromagnetic coupling interactions with a pincer radical anion. A qualitative molecular orbital diagram for (^{tBu}PNP)-CoCH$_3$ is presented in Figure 10, and that for (^{tBu}PNP)CoH is reported in Figure S2 of the Supporting Information. The antiferromagnetic coupling interaction (S = 0.67, X = CH$_3$; S = 0.77, X = H) occurs between an essentially d_{xz} orbital on Co with a ligand b_2 orbital in the SOMO of the pincer. The spin density plots for both (^{tBu}PNP)CoCH$_3$ and (^{tBu}PNP)CoH are presented in Figure 11. It is important to note, however, that the energy differences between the broken symmetry and closed-shell solutions for (^{tBu}PNP)CoCH$_3$ and (^{tBu}PNP)CoH are very small (~1.5 kcal, Table 7) and perhaps within the error limits of the computation. Recall that when RKS solutions are favored, as in the case of (^{tBu}PNP)CoCl and (^{tBu}PNP)CoCCPh, the energy of the broken symmetry solution can not be obtained and the relative energy between the redox active and redox innocent cases for these compounds is unknown. On the

dx.doi.org/10.1021/ja504334a | J. Am. Chem. Soc. 2014, 136, 9211–9224

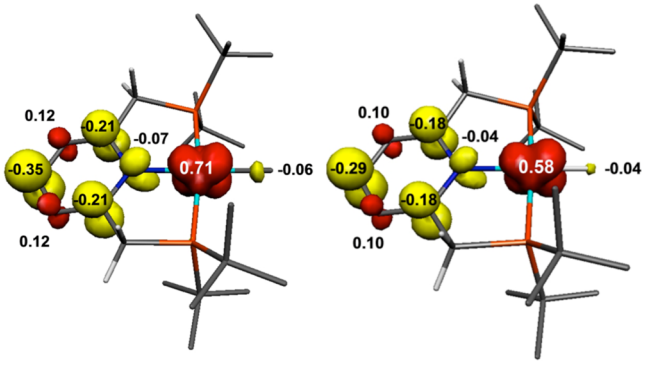

Figure 11. DFT-computed Mulliken spin density plots corresponding to broken-symmetry solutions for (^{tBu}PNP)CoCH$_3$ (left) and (^{tBu}PNP)CoH (right).

Table 7. Electronic Structure and BDFE Correlations for (^{tBu}PNP)CoX Compounds

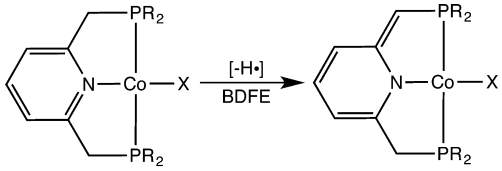

(^{tBu}PNP)CoX (^{tBu}mPNP)CoX

compound	electronic structure	ΔE (kcal) (BS-RKS)	calculated BDFE (kcal)
(^{tBu}PNP)	N/A	N/A	79.8
(^{tBu}PNP)CoCl	RKS	N/A	49.9
(^{tBu}PNP) CoCCPh	RKS	N/A	47.2
(^{tBu}PNP)CoCH$_3$	BS(1,1)	1.4	44.6
(^{tBu}PNP)CoH	BS(1,1)	1.0	42.7
(^{tBu}PNP)RhCl	RKS	N/A	73.7

basis of the combined experimental and computational results, definitive evidence for the radical character on the ^{tBu}PNP ligand is lacking but, as suggested by DFT, should be considered for cases where strong σ-donating ligands are present. Importantly, however, the compounds where broken symmetry solutions were favored undergo thermal H atom loss and have the weakest benzylic C–H bond as established by H atom transfer experiments (Table 6).

The apparent experimental correlation between thermal H atom loss and favored electronic structure prompted a more detailed computational investigation into the homolytic bond dissociation free energies (BDFE) of the benzylic positions of the pincer and the identity of the X-type ligand on cobalt. Table 7 presents the results of DFT-computed (B3LYP functional) BDFEs for the benzylic C–H bond for the four (^{tBu}PNP)CoX complexes. As a reference point, the BDFE of the benzylic positions of the free ligand (^{tBu}PNP) was also calculated and gave a value of 79.8 kcal/mol. For (^{tBu}PNP)CoCl and (^{tBu}PNP)CoCCPh where classical Co(I), d^8 electronic descriptions were computationally preferred, the strongest C–H bonds, 49.9 and 47.2 kcal/mol were calculated. In the cases where broken symmetry descriptions were favored, (^{tBu}PNP)CoCH$_3$ and (^{tBu}PNP)CoH, significantly weaker C–H BDFEs of 44.6 and 42.7 kcal/mol were computed, consistent with the observed thermolysis studies. The DFT-computed C–H BDFEs also rationalize the observations with TEMPO where each complex undergoes H atom abstraction regardless of the identity of X to form the corresponding modified compound and TEMPO-H.

Comparison of Benzylic C–H Bond Dissociation Free Energies (BDFEs) in First Row versus Second Row Transition Metals. The remarkably low BDFEs of the benzylic C–H bonds in (^{tBu}PNP)CoX compounds prompted further investigation into the origin of heterolytic vs homolytic bond cleavage in (^{R}PNP)MX complexes. Although ligand modification is commonly observed in second row transition metal complexes supported by PNP pincer ligands,[2] heterolytic C–H bond cleavage via deprotonation of the ligand framework in conjunction with two-electron redox transformations is the accepted pathway. During the preparation of this manuscript, a rare example of homolytic C–H bond cleavage in a PNN-ligated rhodium complex was reported.[64] To explore this possibility in more detail, the electronic structures of (^{tBu}PNP)-RhCl and its modified derivative (^{tBu}mPNP)RhCl were computed. The homolytic bond dissociation free energies (BDFE) for the benzylic C–H bond of the [^{tBu}PNP] pincer was also calculated. Similar to the cobalt congener, full molecule calculations of (^{tBu}PNP)RhCl established a diamagnetic closed-shell ground state with no indication of a broken-symmetry solution indicating that the compound is best described as a Rh(I) complex with a neutral closed-shell pincer.

For the modified complex, (^{tBu}mPNP)RhCl, the computations yielded a doublet ground state in which the spin density is located predominantly on the metal center (Figure 12). This is

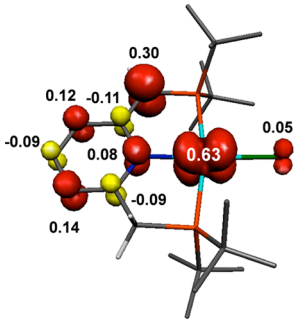

Figure 12. DFT-computed Mulliken spin density plot for (^{tBu}mPNP)-RhCl.

again analogous to the corresponding cobalt congener with the compound best described as a rhodium(II) derivative with an anionic closed-shell pincer. In contrast to the cobalt analogue, however, the SOMO possesses mostly rhodium d_{xz} character (d_{z_2} is the parentage for Co) and exhibits strong covalent interactions with the now extended π system of the PNP ligand. The increased covalency in metal–ligand bonding is expected for the second row metal rhodium, because of its more diffuse 4d orbitals compared to the 3d metal cobalt. Similar trends have previously been reported for a series of isostructural iron and ruthenium dithiolene complexes.[65,66]

After establishing the electronic structures of the relevant compounds, the BDFEs of the benzylic C–H bonds in (^{tBu}PNP)RhCl were computed as 73.7 kcal/mol. This value is slightly lower than the calculated value for the free ligand but is significantly higher than for the cobalt analogue. These results clearly indicate that the nature of the central metal ion has a dramatic influence on the BDFEs of the remote backbone C–H bonds and showcases the differences between first and

dx.doi.org/10.1021/ja504334a | J. Am. Chem. Soc. 2014, 136, 9211–9224

second row transition metals. During the H atom transfer step, the accessible Co(I)−Co(II) one-electron redox couple of the first-row metal engages in single-electron transfer to the ligand, resulting in an oxidized metal center and an overall one-proton, two-electron transformation (net deprotonation) of the ligand. In other words, the heterolytic C−H bond cleavage proceeds via concerted proton−electron transfer (CPET)[67] in which the proton is supplied by the ligand, whereas the electron is supplied by the metal center. In contrast to the first-row metal cobalt, the second-row congener rhodium prefers two-electron chemistry (Rh(I)−Rh(III)) and does not easily engage in single-electron transfer to generate Rh(II). This is clearly reflected in the Rh(I)−Rh(II) redox potential reported previously for (^{tBu}PNP)RhCl, which is shifted by more than 1.5 V compared to the potential reported in this work for (^{tBu}PNP)CoCl rendering oxidation more difficult. These results show that the dramatic difference in C−H BDFEs between Co and Rh can, therefore, be directly attributed to the tendency of first-row metals to undergo one-electron redox processes.

Experimental support was sought for the higher computed C−H BDFE of (^{tBu}PNP)RhCl. As anticipated, treatment of a benzene-d_6 solution of (^{tBu}PNP)RhCl with one equivalent of TEMPO produced no reaction, even upon heating to 80 °C. In contrast, addition of the sterically encumbered 2,4,6-tri(*tert*-butyl)phenoxy radical with a BDFE of 76.7 kcal/mol in benzene,[56] proved capable of abstracting a H atom from the PNP chelate, generating one equivalent of 2,4,6-tri(*tert*-butyl)phenol and (^{tBu}mPNP)RhCl (eq 5).

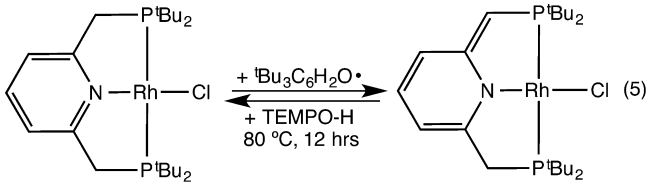

(^{tBu}PNP)RhCl (^{tBu}mPNP)RhCl

These data confirm the computed BDFE and provide convincing experimental support for the influence of a first versus a second row transition metal on the properties of a coordinated ligand. The reverse reaction, H atom addition to the benzylic position of (^{tBu}mPNP)RhCl was also studied. Heating a benzene-d_6 solution of (^{tBu}mPNP)RhCl in the presence of excess TEMPO-H to 80 °C for 12 h resulted in reconstitution of (^{tBu}PNP)RhCl, also in agreement with the computed BDFE for this position. Repeating this procedure with TEMPO−D furnished (^{tBu}PNP-d_1)RhCl with the isotopic label located exclusively at the benzylic position in the diamagnetic product.

CONCLUDING REMARKS

A series of four-coordinate, *tert*-butyl substituted pincer cobalt complexes, (^{tBu}PNP)CoX, were isolated and their electronic structures and thermal stability systematically evaluated. Modification of the benzylic positions of the pincer by both heterolytic and homolytic C−H bond cleavage proved feasible with deprotonation pathways likely operative in previous literature reports. The electronic structure of the resulting modified pincer cobalt complexes, (^{tBu}mPNP)CoX was established by EPR spectroscopy, magnetometry and computational studies as low-spin cobalt(II) complexes with a closed-shell anionic form of the modified chelate. The homolytic bond dissociation free energies of the benzylic C−H bonds of the (^{tBu}PNP)CoX complexes were computed by DFT and range between 42.7 and 49.9 kcal/mol, depending on the identity of the X-type ligand where pure σ donors such as hydride and methyl generate the weakest C−H bonds. These values were experimentally corroborated by abstraction with TEMPO and by H atom transfer experiments between cobalt complexes. The origin of the relatively weak C−H bonds in these compounds was traced to the energetically accessible one-electron redox couple, for example, Co(I)−Co(II) of the first row transition metal. In contrast, the second row congener, (^{tBu}PNP)RhCl, has a much higher thermodynamic barrier to one-electron redox chemistry, and as such much, stronger pincer C−H bonds are observed.

EXPERIMENTAL SECTION[68]

Preparation of (^{tBu}PNP)CoCl. A 100 mL round-bottom flask was charged with 0.409 g (0.779 mmol) of (^{tBu}PNP)CoCl$_2$ and 25 mL of toluene. The solution was frozen in the cold well of the glovebox. To the thawing suspension was added 780 μL (0.779 mmol) of a 1.0 M NaHBEt$_3$ solution in toluene dropwise via syringe. A color change from dark purple to red-orange was observed immediately upon warming to 23 °C. The reaction mixture was stirred for 12 h at 23 °C followed by filtration through Celite. Recrystallization of the crude material from a toluene-pentane mixture at −35 °C furnished 0.252 g (0.514 mmol, 66% yield) of red-brown crystals suitable for X-ray diffraction. Anal. Calcd for $C_{23}H_{43}ClCoNP_2$: C, 56.39; H, 8.85; N, 2.86. Found: C, 56.23; H, 8.58; N, 2.93. ^{1}H NMR (benzene-d_6, 23 °C): δ 1.59 (br s, 36 H, P−CMe_3), 1.69 (br s, 4H, P−CH_2), 5.60 (d, $^3J_{HH}$ = 7.2 Hz, 2H, meta aryl CH), 7.69 (t, 1H, $^3J_{HH}$ = 7.2 Hz, para aryl CH). {^{1}H}^{13}C NMR (benzene-d_6, 23 °C): δ 30.0 (P−CMe_3), 34.6 (br s, P-CH_2), 35.6 (br s, P-CMe_3), 116.3 (meta aryl *C*), 122.3 (br m, *para*-aryl *C*), 160.6 (br m, ipso aryl *C*). {^{1}H}^{31}P NMR (benzene-d_6, 23 °C): δ 54.9 (br m, *P*(tBu)$_2$).

Preparation of (^{tBu}mPNP)CoCl. A 20 mL scintillation vial was charged with 0.148 g (0.302 mmol) of (^{tBu}PNP)CoCl and 3 mL of diethyl ether. To the stirring solution was added dropwise a solution containing 0.045 g (0.302 mmol) of 2,2,6,6-tetramethylpiperidine-*N*-oxide (TEMPO) in 1 mL of diethyl ether. An immediate lightening of the solution from red-brown to orange was observed upon addition of TEMPO. The solution was stirred overnight at room temperature before the solution was filtered through Celite to remove excess 1-hydroxy-2,2,6,6-tetramethylpiperidine (TEMPO-H). The filtrate was concentrated in vacuo and recrystallized at −35 °C and yielded 0.118 g (0.242 mmol, 80% yield) of dark red-orange crystals suitable for X-ray diffraction identified as (^{tBu}mPNP)CoCl. Anal. Calcd for $C_{23}H_{42}ClCoNP_2$: C, 56.50; H, 8.65; N, 2.86. Found: C, 56.54; H, 8.70; N, 2.68. ^{1}H NMR (benzene-d_6, 23 °C): δ −55.6 (1H, $\Delta\nu_{1/2}$ = 562 Hz), −47.8 (1H, $\Delta\nu_{1/2}$ = 312 Hz), −30.4 (1H, $\Delta\nu_{1/2}$ = 293 Hz), −0.87 (1H, $\Delta\nu_{1/2}$ = 26 Hz), 1.36 (2H, $\Delta\nu_{1/2}$ = 33 Hz, P−CH_2), 9.22 (18H, $\Delta\nu_{1/2}$ = 514 Hz, P−CMe_3), 12.55 (18H, $\Delta\nu_{1/2}$ = 514, P−CMe_3). Magnetic susceptibility: (benzene-d_6, 23 °C) μ_{eff} = 1.6(5) μ_B.

Preparation of (^{tBu}PNP)CoH. This compound was prepared in a similar manner to (^{tBu}PNP)CoCl using 0.250 g (0.476 mmol) of (^{tBu}PNP)CoCl$_2$ and 952 μL (0.952 mmol) of a 1.0 M NaHBEt$_3$ solution in toluene. Upon warming to 23 °C, a color change from dark purple to red-orange was observed. Following work-up, recrystallization of the crude material from diethyl ether at −35 °C furnished 0.150 g (0.328 mmol, 69% yield) of red-brown crystals suitable for X-ray diffraction identified as (^{tBu}PNP)CoH. Anal. Calcd for $C_{23}H_{44}CoNP_2$: C, 60.65; H, 9.74; N, 3.08. Found: C, 60.33; H, 9.59; N, 3.05. ^{1}H NMR (benzene-d_6, 23 °C): δ −29.0 (t, $^2J_{PH}$ = 65.3 Hz, 1H, Co-*H*), 1.45 (AA′XX′, 36 H, P−CMe_3), 1.84 (m, 4H, P−CH_2), 5.77 (d, $^3J_{HH}$ = 7.2 Hz, 2H, meta aryl CH), 8.93 (br m, 1H, para aryl CH). {^{1}H}^{13}C NMR (benzene-d_6, 23 °C): δ 30.2 (m, P−CMe_3), 33.8 (m, P-CH_2), 38.0 (m, P-CMe_3), 110.2 (br m, meta aryl *C*), 124.1 (para aryl *C*), 155.6 (br m, ipso aryl *C*). {^{1}H}^{31}P NMR (benzene-d_6, 23 °C): δ 85.2 (br s, *P*(tBu)$_2$). IR (KBr): ν_{Co-H} = 1746 cm^{-1}.

dx.doi.org/10.1021/ja504334a | J. Am. Chem. Soc. 2014, 136, 9211−9224

■ ASSOCIATED CONTENT

Supporting Information

Additional experimental procedures, including general considerations and characterization data, as well as computational and spectroscopic results. Crystallographic data for (^{tBu}PNP)-$CoCH_3$, (^{tBu}PNP)CoCl, (^{tBu}PNP)CoH, (^{tBu}mPNP)CoCl, (^{tBu}mPNP)CoH, (^{tBu}mPNP)CoN_2, (^{tBu}PNP)Co(C_6H_4−CH═CHPh), and (^{tBu}PNP)CoCCPh in .txt format. This material is available free of charge via the Internet at http://pubs.acs.org.

■ AUTHOR INFORMATION

Corresponding Author

pchirik@princeton.edu

Author Contributions

†These authors contributed equally to this work.

Notes

The authors declare no competing financial interest.

■ ACKNOWLEDGMENTS

Princeton University is acknowledged for financial support. Initial studies were enabled by financial support from the U. S. National Science Foundation and the Deutsche Forschungsgemeinschaft for a Cooperative Activities in Chemistry between U. S. and German Investigators Grant (CHE-1026084). Support for C.M. was provided by the Air Force Office of Scientific Research (FA9550-11-1-0252) and we thank Dr. Eckhard Bill (Max Planck Institute for Chemical Energy Conversion) for assistance in interpreting the EPR spectra.

■ REFERENCES

(1) *The Chemistry of Pincer Compounds*; Morales-Morales, D., Jensen, C. M., Eds.; Elsevier: Amsterdam, 2007.
(2) Gunanathan, C.; Milstein, D. *Acc. Chem. Res.* **2011**, *44*, 588.
(3) Haneline, M. R.; Heyduk, A. F. *J. Am. Chem. Soc.* **2006**, *128*, 8410.
(4) Chirik, P. J.; Weighardt, K. *Science* **2010**, *327*, 794.
(5) Mazzacano, T. J.; Mankad, N. P. *J. Am. Chem. Soc.* **2013**, *135*, 17258.
(6) Grutzmacher, H.-J. *Angew. Chem., Int. Ed.* **2008**, *47*, 1814.
(7) Vogt, M.; Gargir, M.; Iron, M. A.; Diskin-Posner, Y.; Ben-David, Y.; Milstein, D. *Chem.—Eur. J.* **2012**, *18*, 9194.
(8) Bichler, B.; Holzhacker, C.; Stoger, B.; Puchberger, M.; Veiros, L. F.; Kirchner, K. *Organometallics* **2013**, *32*, 4414.
(9) Alberico, E.; Sponholz, P.; Cordes, C.; Nielsen, M.; Drexler, H.-J.; Baumann, W.; Junge, H.; Beller, M. *Angew. Chem., Int. Ed.* **2013**, *52*, 14162.
(10) Monfette, S.; Turner, Z. R.; Semproni, S. P.; Chirik, P. J. *J. Am. Chem. Soc.* **2012**, *134*, 4561.
(11) Prokopchuk, D. E.; Morris, R. *Organometallics* **2012**, *31*, 7375.
(12) Mikhailine, A. A.; Maishan, M. I.; Lough, A. J.; Morris, R. H. *J. Am. Chem. Soc.* **2012**, *134*, 12266.
(13) Bauer, G.; Kirchner, K. A. *Angew. Chem., Int. Ed.* **2011**, *50*, 5798.
(14) Langer, R.; Iron, M. A.; Lonstantinovski, L.; Diskin-Posner, Y.; Leitus, G.; Ben-David, Y.; Milstein, D. *Chem.—Eur. J.* **2012**, *18*, 7196.
(15) Casey, C. P.; Guan, H. *J. Am. Chem. Soc.* **2007**, *129*, 5816.
(16) Zou, W.; Lough, A. J.; Li, Y. F.; Morris, R. H. *Science* **2013**, *342*, 1080.
(17) Clapham, S. E.; Hadzovic, A.; Morris, R. H. *Coord. Chem. Rev.* **2004**, *248*, 2201.
(18) Ikariya, T.; Blacker, A. J. *Acc. Chem. Res.* **2007**, *40*, 1300.
(19) Tanaka, R.; Yamashita, M.; Nozaki, K. *J. Am. Chem. Soc.* **2009**, *131*, 14168.
(20) Langer, R.; Diskin-Posner, Y.; Leitus, G.; Shimon, L. J. W.; Ben-David, Y.; Milstein, D. *Angew. Chem., Int. Ed.* **2011**, *50*, 9948.
(21) Milstein, D. *Top. Catal.* **2010**, *53*, 915.
(22) (a) Zhang, J.; Leitus, G.; Ben-David, Y.; Milstein, D. *J. Am. Chem. Soc.* **2005**, *127*, 10840. (b) Gunanathan, C.; Ben-David, Y.; Milstein, D. *Science* **2007**, *317*, 790. (c) Gnanaprakasam, B.; Zhang, J.; Milstein, D. *Angew. Chem., Int. Ed.* **2010**, *48*, 1468. (d) Gnanaprakasam, B.; Milstein, D. *J. Am. Chem. Soc.* **2011**, *133*, 1682.
(23) Käss, M.; Friedrich, A.; Dress, M.; Schneider, S. *Angew. Chem., Int. Ed.* **2009**, *48*, 905.
(24) Knijnenburg, Q.; Gambarotta, S.; Budzelaar, P. H. M. *Dalton Trans.* **2006**, 5442.
(25) Chirik, P. J. *Inorg. Chem.* **2011**, *50*, 9737.
(26) Tellman, K. P.; Humphries, M. J.; Rzepa, H. S.; Gibson, V. C. *Organometallics* **2004**, *23*, 5503.
(27) Knijnenburg, Q.; Hetterscheid, D.; Kooistra, T. M.; Budzelaar, P. H. M. *Eur. J. Inorg. Chem.* **2004**, 1204.
(28) Bowman, A. C.; Milsmann, C.; Atienza, C. C. H.; Lobkovsky, E.; Wieghardt, K.; Chirik, P. J. *J. Am. Chem. Soc.* **2010**, *132*, 1676.
(29) Knijnenburg, Q.; Horton, A. D.; van der Heijden, H.; Kooistra, T. M.; Hetterscheid, D. G. H.; Smits, J. M. M.; de Bruin, B.; Budzelaar, P. H. M.; Gal, A. W. *J. Mol. Catal. A: Chem.* **2005**, *232*, 151.
(30) Obligacion, J. V.; Chirik, P. J. *J. Am. Chem. Soc.* **2013**, *135*, 19107.
(31) Yu, R. P.; Darmon, J. M.; Hoyt, J. M.; Margulieux, G. W.; Turner, Z. R.; Chirik, P. J. *ACS Catal.* **2012**, *2*, 1760.
(32) Atienza, C. C. H.; Tondreau, A. M.; Weller, K. J.; Lewis, K. M.; Cruse, R. W.; Nye, S. A.; Boyer, J. L.; Delis, J. G. P.; Chirik, P. J. *ACS Catal.* **2012**, *2*, 2169.
(33) Danopoulos, A. A.; Wright, J. A.; Motherwell, W. B.; Ellwood, S. *Organometallics* **2004**, *23*, 4807.
(34) Yu, R. P.; Darmon, J. M.; Milsmann, C.; Margulieux, G. W.; Stieber, S. C. E.; DeBeer, S.; Chirik, P. J. *J. Am. Chem. Soc.* **2013**, *135*, 13168.
(35) Zhang, G.; Scott, B. L.; Hanson, S. K. *Angew. Chem., Int. Ed.* **2012**, *51*, 12102.
(36) Zhang, G.; Hanson, S. K. *Org. Lett.* **2013**, *15*, 650.
(37) Zhang, G.; Vasudevan, K. V.; Scott, B. L.; Hanson, S. K. *J. Am. Chem. Soc.* **2013**, *135*, 8668.
(38) (a) Moulton, C. J.; Shaw, B. L. *J. Chem. Soc., Dalton Trans.* **1976**, 1020. (b) Gupta, M.; Hagen, C.; Flesher, R. J.; Kaska, W. C.; Jensen, C. M. *Chem. Commun.* **1996**, 2083. (c) van der Boom, M. E.; Milstein, D. *Chem. Rev.* **2003**, *103*, 1759.
(39) van der Vlugt, J. L.; Reek, J. N. H. *Angew. Chem., Int. Ed.* **2009**, *48*, 8832.
(40) Gunanathan, C.; Gnanaprakasam, B.; Iron, M. A.; Shimon, L. J. W.; Milstein, D. *J. Am. Chem. Soc.* **2010**, *132*, 14763.
(41) Kloek, S. M.; Heinekey, D. M.; Goldberg, K. I. *Angew. Chem., Int. Ed.* **2007**, *46*, 4736.
(42) Blanksby, S. J.; Ellison, G. B. *Acc. Chem. Res.* **2003**, *36*, 255.
(43) Trovitch, R. J.; Lobkovsky, E.; Chirik, P. J. *Inorg. Chem.* **2006**, *45*, 7252.
(44) Pelczar, E. M.; Emge, T. J.; Krogh-Jespersen, K.; Goldman, A. S. *Organometallics* **2008**, *27*, 5759.
(45) Danopoulos, A. A.; Wright, J. A.; Motherwell, W. B. *Chem. Commun.* **2005**, 784.
(46) For related iron carbonyl compounds with bis(phosphine) pyridine pincers with amino rather than methylene linkers see: Bichler, B.; Holzhacker, C.; Stöger; Puchberger, M.; Veiros, L. F.; Kirchner, K. *Organometallics* **2013**, *32*, 4114.
(47) Semproni, S. P.; Atienza, C. C. H.; Chirik, P. J. *Chem. Sci.* **2014**, *5*, 1956.
(48) For related H_2 oxidative addition chemistry with cobalt pincers see: Rozenel, S. S.; Padilla, R.; Camp, C.; Arnold, J. *Chem. Commun.* **2014**, *50*, 2612.
(49) Obligacion, J. V.; Semproni, S. P.; Chirik, P. J. *J. Am. Chem. Soc.* **2014**, *136*, 4133.
(50) Khaskin, E.; Diskin-Posner, Y.; Weiner, L.; Leitus, G.; Milstein, D. *Chem. Commun.* **2013**, 2771.
(51) Kaesz, H. D.; Saillant, R. B. *Chem. Rev.* **1972**, *72*, 233.

(52) Feller, M.; Ben-Ari, E.; Gupta, T.; Shimon, L. J. W.; Leitus, G.; Diskin-Posner, E.; Weiner, L.; Milstein, D. *Inorg. Chem.* **2007**, *46*, 10479.
(53) Atienza, C. C. H.; Milsmann, C.; Semproni, S. P.; Turner, Z. R.; Chirik, P. J. *Inorg. Chem.* **2013**, *52*, 5403.
(54) Ben-Ari, E.; Leitus, G.; Shimon, L. J. W.; Milstein, D. *J. Am. Chem. Soc.* **2006**, *128*, 15390.
(55) Warren, J. J.; Tronic, T. A.; Mayer, J. M. *Chem. Rev.* **2010**, *110*, 6961.
(56) (a) Maki, A. H.; Edelstein, N.; Davison, A.; Holm, R. H. *J. Am. Chem. Soc.* **1964**, *86*, 4580. (b) Nishida, Y.; Sumita, A.; Kida, S. *Bull. Chem. Soc. Jpn.* **1977**, *50*, 759143. (c) Nishida, Y.; Kida, S. *Bull. Chem. Soc. Jpn.* **1978**, *51*, 143. (d) Nishida, Y.; Hayashi, K.; Sumita, A.; Kida, S. *Bull. Chem. Soc. Jpn.* **1980**, *53*, 271.
(57) Przyojski, J. A.; Arman, H. D.; Tonzetich, Z. J. *Organometallics* **2013**, *32*, 723.
(58) Lazzaro, D. P.; Fanwick, P. E.; McMillin, D. R. *Inorg. Chem.* **2012**, *51*, 10474.
(59) Vuzman, D.; Poverenov, E.; Shimon, L. J. W.; Diskin-Posner, Y.; Milstein, D. *Organometallics* **2008**, *27*, 2627.
(60) (a) van der Vlugt, J. I.; Siegler, M. A.; Janssen, M.; Vogt, D.; Spek, A. L. *Organometallics* **2009**, *28*, 7025. (b) Feller, M.; Ben-Ari, E.; Iron, M. A.; Diskin-Posner, Y.; Leitus, G.; Shimon, L. J. W.; Konstantinovski, L.; Milstein, D. *Inorg. Chem.* **2010**, *49*, 1615.
(61) (a) Vogt, M.; Rivada-Wheelaghan, O.; Iron, M. A.; Leitus, G.; Diskin-Posner, Y.; Shimon, L. J. W.; Ben-David, Y.; Milstein, D. *Organometallics* **2013**, *32*, 300. (b) van der Vlugt, J. I.; Lutz, M.; Pidko, E. A.; Vogt, D.; Spek, A. L. *Dalton Trans.* **2009**, 1016.
(62) van der Vlugt, J. I.; Pidko, E. A.; Bauer, R. C.; Gloaguen, Y.; Rong, M. K.; Lutz, M. *Chem.—Eur. J.* **2011**, *17*, 3850.
(63) Neese, F. *Orca - an ab initio, DFT and Semiempirical Electronic Structure Package*, Version *2.8*, Revision 2287; Institut für Physikalische und Theoretische Chemie, Universität Bonn: Bonn (Germany), 2010.
(64) Gloaguen, Y.; Rebreyend, C.; Lutz, M.; Kumar, P.; Huber, M.; Schneider, S.; de Bruin, B. *Angew. Chem., Int. Ed.* **2014**, No. 10.1002/anie.201403445.
(65) Milsmann, C.; Patra, G. K.; Bill, E.; Weyhermüller, T.; DeBeer George, S.; Wieghardt, K. *Inorg. Chem.* **2009**, *48*, 7430.
(66) Milsmann, C.; Bill, E.; Weyhermüller, T.; DeBeer George, S.; Wieghardt, K. *Inorg. Chem.* **2009**, *48*, 9754.
(67) Warren, J. J.; Tronic, T. A.; Mayer, J. M. *Chem. Rev.* **2010**, *110*, 6961.
(68) Only representative procedures are reported here. Full experimental details, including General Considerations, are reported in the Supporting Information.